

Rare heavy flavour decays at LHCb

Flavio Archilli^{*†}

Laboratori Nazionali dell'INFN di Frascati, Frascati, Italy

E-mail: flavio.archilli@cern.ch

Rare lepton decays of the $B_{(s)}^0$ and D mesons are sensitive probes of New Physics. In particular, the search for the decays $B_{(s)}^0 \rightarrow \mu^+ \mu^-$ may provide information on the presence of new (pseudo-)scalar particles. The LHCb experiment is well suited for these analyses due to its large acceptance and trigger efficiency, as well as its excellent invariant mass resolution and lepton identification capabilities. The status of these analyses with $\sim 1 \text{ fb}^{-1}$ of pp collisions collected by LHCb in 2011 at $\sqrt{s} = 7 \text{ TeV}$ is reviewed.

*The XIth International Conference on Heavy Quarks and Leptons,
June 11-15, 2012
Prague, Czech Republic*

^{*}Speaker.

[†]on behalf of the LHCb collaboration.

1. Introduction

The study of rare B and D decays is a complementary approach to detect New Physics (NP) with respect to the direct searches. New particles can enter as virtual particles in loop diagrams and their effects can be observed as a deviation in the Standard Model (SM) expectation for observables such as branching ratio, angular distribution, either in CP violating processes or in very rare decays involving Flavour Changing Neutral Current (FCNC). These decays are mediated by penguin and box diagrams and therefore receive very small contribution in the SM. In this case, New Physics (NP) effects can then be of the same order or even higher than the SM contribution.

Hadronic weak decays can be studied in terms of an effective Hamiltonian of local operator \mathcal{O}_i

$$H_{\text{eff}} \propto \sum_i \mathcal{C}_i \mathcal{O}_i$$

where the degrees of freedom of exchanged particles are integrated out, giving rise to the Wilson coefficients \mathcal{C}_i . These terms, depending on the underlying physics model and can be modified by NP effects.

2. $B_{(s)}^0 \rightarrow \mu^+ \mu^-$

The search for $B_{(s)}^0 \rightarrow \mu^+ \mu^-$ is one of the most promising ways for the LHCb experiment to constrain the parameters of any extended Higgs sector. These decays are highly suppressed in the SM because they are both FCNC and helicity suppressed. The amplitude can be expressed using scalar (\mathcal{C}_S), pseudoscalar (\mathcal{C}_P) and axial vector (\mathcal{C}_A) Wilson coefficients. The first two are negligible in the SM while the last one is accurately evaluated at the level of a few percent. The SM model predictions for these decays are [1]:

$$\begin{aligned} \mathcal{B}(B_s^0 \rightarrow \mu^+ \mu^-)_{SM} &= (3.2 \pm 0.2) \times 10^{-9} \\ \mathcal{B}(B^0 \rightarrow \mu^+ \mu^-)_{SM} &= (1.0 \pm 0.1) \times 10^{-10} \end{aligned}$$

Many extensions of the SM predict large enhancements to these branching fractions. If we consider the Minimal Supersymmetric SM (MSSM) in the large $\tan\beta$ approximation $\mathcal{C}_{S,P}^{MSSM} \approx \tan^3 \beta / M_A^2$ and $\mathcal{B}(B_s^0 \rightarrow \mu^+ \mu^-)$ is found to be approximately proportional to $\tan^6 \beta$ [2], where $\tan\beta$ is the ratio of the vacuum expectation values of the two neutral CP-even Higgs fields and M_A is the pseudoscalar Higgs mass. The branching fractions could therefore be enhanced by orders of magnitude for large values of $\tan\beta$.

The CDF collaboration observes an excess of $B_s^0 \rightarrow \mu^+ \mu^-$ using a dataset of 7 fb^{-1} compatible with $\mathcal{B}(B_s^0 \rightarrow \mu^+ \mu^-) = (1.8_{-0.9}^{+1.1}) \times 10^{-8}$ [6]. The CMS collaboration, using a sample of 4.9 fb^{-1} , has measured $\mathcal{B}(B_s^0 \rightarrow \mu^+ \mu^-) < 7.7 \times 10^{-9}$ and $\mathcal{B}(B^0 \rightarrow \mu^+ \mu^-) < 1.8 \times 10^{-9}$ at 95% C.L. [7]. The previous LHCb published limits based on 370 pb^{-1} are $\mathcal{B}(B_s^0 \rightarrow \mu^+ \mu^-) < 1.6 \times 10^{-8}$ and $\mathcal{B}(B^0 \rightarrow \mu^+ \mu^-) < 3.2 \times 10^{-9}$ at 95% C.L. [9].

The results presented here is based on $\sim 1.0 \text{ fb}^{-1}$ of data recorded by LHCb in 2011. This dataset includes the 370 pb^{-1} used for the previous published limit [3]. To separate signal from background, the analysis uses a multivariate classifier, a boosted decision tree (BDT), based on kinematic and geometrical variables used to increase the signal and background separation. The

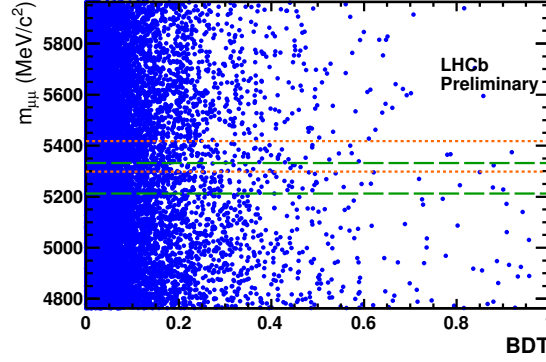


Figure 1: Unblinded data: 2D plot of mass versus BDT. Orange short-dashed (green long-dashed) lines indicate the $\pm 60 \text{ MeV}/c^2$ search window around the B_s^0 (B^0).

Mode	ATLAS	CMS	LHCb	Combined
$\mathcal{B}(B_s^0 \rightarrow \mu^+ \mu^-) (10^{-9})$	22	7.7 (7.2)	4.5	4.2
$\mathcal{B}(B^0 \rightarrow \mu^+ \mu^-) (10^{-10})$	-	14 (16)	10	8.1

Table 1: Observed upper limit at 95% C.L. on $\mathcal{B}(B_{(s)}^0 \rightarrow \mu^+ \mu^-)$ published by each experiment and their combination. For CMS, the numbers in parentheses correspond to the analysis used in the combination.

events are classified in a bi-dimensional plane (Fig.1) of the dimuon invariant mass ($m_{\mu\mu}$) and BDT. The plane has been divided into 72 bins and for each bin the expected signal and background yields are computed. The number of expected signal events, for a given branching ratio hypothesis, is evaluated by normalizing to the decays $B_d \rightarrow K\pi$, $B^+ \rightarrow J/\psi K^+$ and $B_s \rightarrow J/\psi \phi$.

The compatibility of the observed events with background-only and background plus signal hypothesis is then computed. The modified frequentist method CL_s is used for the upper limit extraction [4]. In order to avoid any bias, the mass region $m_{\mu\mu} = [m(B^0) - 60 \text{ MeV}/c^2, m(B_s^0) + 60 \text{ MeV}/c^2]$ is blinded until the analysis is finalized.

The upper limit obtained are:

$$\begin{aligned} \mathcal{B}(B_s^0 \rightarrow \mu^+ \mu^-) &< 4.5 \times 10^{-9} \\ \mathcal{B}(B^0 \rightarrow \mu^+ \mu^-) &< 1.03 \times 10^{-9} \end{aligned}$$

both evaluated at 95% of C.L.. In order to compare the upper limit on $\mathcal{B}(B_s^0 \rightarrow \mu^+ \mu^-)$ with the theoretical prediction, this value has to be multiplied by 0.911 ± 0.014 , which takes into account the effective lifetime of the B_s meson [5]. The CL_s curves for $\mathcal{B}(B^0 \rightarrow \mu^+ \mu^-)$ and $\mathcal{B}(B_s^0 \rightarrow \mu^+ \mu^-)$ are shown in Fig.2.

These two upper limits have been also recently combined [10] with the result obtained by CMS with 4.9 fb^{-1} [7] and ATLAS with 2.9 fb^{-1} [8]. The combined upper limits obtained by each experiments are shown in Table 1.

In Fig.3 the CL_s curves from the combination are shown. The results are compatible with the SM prediction and NP enhancements of $\mathcal{B}(B_s^0 \rightarrow \mu^+ \mu^-)$ are constrained to be of the same order of the SM prediction. However, there is still room for contributions from physics beyond the SM. For

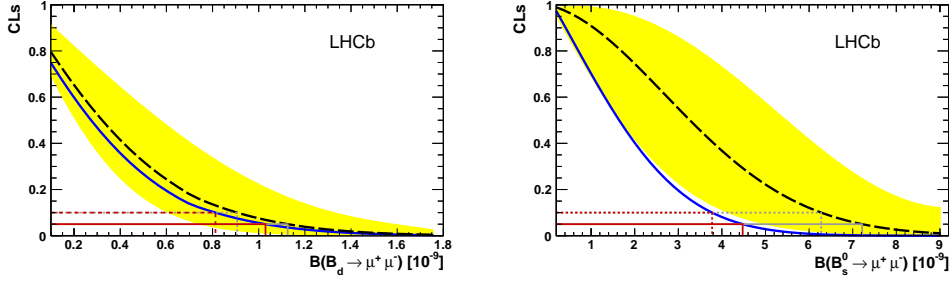


Figure 2: Expected CL_s (dashed black line) under the hypothesis to observe background-only (left) for the $B^0 \rightarrow \mu^+ \mu^-$ and CL_s under background-plus-signal events according to the SM rate (right) for $B_s^0 \rightarrow \mu^+ \mu^-$, with yellow area covering the region of $\pm 1\sigma$ of compatible observations; the observed CL_s is given by the blue dotted line; the expected (observed) upper limits at 90% and 95% C.L. are also shown as dashed and solid grey (red) lines.

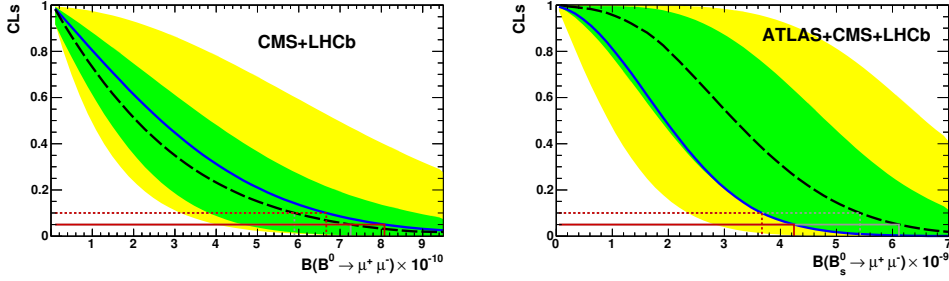


Figure 3: CL_s as a function of the assumed branching fraction for $B^0 \rightarrow \mu^+ \mu^-$ (left) and $B_s^0 \rightarrow \mu^+ \mu^-$ (right) obtained from the combination of LHCb CMS and ATLAS. The long dashed black curves are the medians of the expected CL_s distributions, in case of background-only (left) or background plus signal according to the SM rate (right). The green (yellow) areas cover, for each branching fraction, corresponding to $\pm 1(2)\sigma$ intervals. The solid blue curves are the observed CL_s . The upper limits at 90% (95%) C.L. are indicated by the dotted (solid) horizontal lines in red (dark grey) for the observation and in grey for the expectation.

example, destructive interference between NP and the SM could decrease significantly the value of the branching ratio.

3. $D^0 \rightarrow \mu^+ \mu^-$

The $D^0 \rightarrow \mu^+ \mu^-$ decay is very rare in the SM. Its branching fraction is dominated by the long distance contribution due to two-photon intermediate state which implies a lower bound of the SM contribution from the vector meson dominance mechanism and an upper bound due to the best experimental upper limit on $\mathcal{B}(D^0 \rightarrow \gamma\gamma)$. Therefore the SM prediction is in the range $10^{-13} < \mathcal{B} < 6 \times 10^{-11}$ at 90% C.L. [11]. Enhancements are predicted in many NP models, e.g. RPV-SUSY, which predicts $\mathcal{B} \sim 10^{-9}$ due to a tree level transition [12]) The current best experimental limit is $\mathcal{B} < 1.4 \times 10^{-7}$ at 90% C.L., from Belle [13]

An analysis using LHCb data has been performed on a data sample of 0.9 fb^{-1} and selecting the decay chain $D^{*\pm} \rightarrow D^0(\rightarrow \mu^+ \mu^-) \pi^\pm$ decays. The selection of the events is based on geometric and kinematic properties of D^0 and its daughter particles. The same selection is applied to signal and control channels. After this selection the background is mainly composed

of combinatorial muons from semileptonic decays of b and c hadrons and the peaking background of $D^{*\pm} \rightarrow D^0(\rightarrow h^+h^-)\pi^\pm$ events, with double hadron misidentification. In order to reduce the combinatorial background, a multivariate discriminant is built based on geometrical and kinematical information. The number of signal events has been obtained by normalizing to the $D^{*\pm} \rightarrow D^0(\rightarrow \pi^+\pi^-)\pi^\pm$ channel and the branching fraction has been evaluated using the following formula:

$$\mathcal{B}(D^0 \rightarrow \mu^+\mu^-) = \frac{N_{D^{*+} \rightarrow D^0(\rightarrow \mu^+\mu^-)\pi^+} \varepsilon_{\pi\pi}}{N_{D^{*+} \rightarrow D^0(\rightarrow \pi^+\pi^-)\pi^+} \varepsilon_{\mu\mu}} \times \mathcal{B}(D^0 \rightarrow \pi^+\pi^-)$$

where N_f is the number of observed events in the final state f , and ε_f is the total selection efficiency. Since the normalization and the signal channels have the same kinematics most of the selection systematic effects cancel out. The event yield is extracted from a 2D fit on the dimuon invariant mass and the difference between the D^{*+} mass and D^0 mass. A preliminary result is given: $\mathcal{B}(D^0 \rightarrow \mu^+\mu^-) < 1.3 \times 10^8$ at 95% C.L. [14].

4. $B_{(s)}^0 \rightarrow \mu^+\mu^-\mu^+\mu^-$

The $B_{(s)}^0 \rightarrow \mu^+\mu^-\mu^+\mu^-$ is a FCNC process and takes its largest contribution from the resonant decay $B_S \rightarrow J/\psi\phi$ in which both mesons decay to two muons. A non-resonant process can also occur in the SM with a virtual photon exchange with a branching ratio not exceeding 10^{-10} [15]. However, NP effects might enhance the $B_{(s)}^0 \rightarrow \mu^+\mu^-\mu^+\mu^-$ branching fraction through the exchange of new particles at tree level.

A cut-based selection has been designed on the 1 fb^{-1} data sample collected during the year 2011. The resonant decay mode has been used to tune the selection algorithm. The signal region has been kept blind until the analysis was optimized. The combinatorial background was estimated from the mass sidebands. The selection criteria for signal and control channels are based on particle identification (PID), separation between the B vertex and the primary vertex, the quality of the B decay vertex. A veto on ϕ and B^+ masses is applied in order to exclude $B^+ \rightarrow J/\psi K^+$ and $B \rightarrow K^*\phi$. All the non-resonant peaking background yields in the signal region are found to be negligible.

The signal branching fraction was measured by normalizing to $B_S^0 \rightarrow J/\psi(\rightarrow \mu^+\mu^-)K^{*0}(\rightarrow K^+\pi^-)$ decays selected with the same criteria. Systematic errors are taken into account comparing Monte Carlo (MC) simulation and data.

After unblinding, one event is observed in the B_d signal window and no events are observed in the B_s window. These measurements are consistent with the expected background yields. The CL_s modified frequentist method has been used to evaluate the compatibility with a given branching fraction hypothesis. The upper limits at 95% C.L. are [16]:

$$\begin{aligned} \mathcal{B}(B_{(s)}^0 \rightarrow \mu^+\mu^-\mu^+\mu^-) &< 1.3 \times 10^{-8} \\ \mathcal{B}(B^0 \rightarrow \mu^+\mu^-\mu^+\mu^-) &< 5.4 \times 10^{-9} \end{aligned}$$

5. Angular analysis of the $B^0 \rightarrow K^{*0} \mu^+ \mu^-$ decay

The rare decay $B^0 \rightarrow K^{*0} \mu^+ \mu^-$ is a sensitive probe for right handed currents and new scalar and pseudoscalar couplings (\mathcal{C}_7 and $\mathcal{C}_{9,10}$) [17]. These NP contributions can effect the angular distributions of the B^0 daughter particles.

The differential decay distribution of the $B^0 \rightarrow K^{*0} \mu^+ \mu^-$ process can be described with three angles, the helicity angle of the kaon, θ_K , the helicity angle of the μ^+ , θ_ℓ , the angle between the decay planes of the dimuon and K^{*0} systems in the B^0 rest frame, ϕ , and the dimuon mass q^2 . Using the folded ϕ angle, $\hat{\phi}^1$, the decay distribution can be parametrized using four observables, A_{FB} , F_L , S_3 [17] and A_{Im} [18] as follows:

$$\frac{1}{\Gamma} \frac{d^4\Gamma}{d\cos\theta_\ell d\theta_K d\hat{\phi} dq^2} = \frac{9}{16\pi} \left[F_L \cos^2 \theta_K + \frac{3}{4} (1 - F_L) (1 - \cos^2 \theta_K) + \right. \\ \left. F_L \cos^2 \theta_K (2 \cos^2 \theta_\ell - 1) + \right. \\ \left. \frac{1}{4} (1 - F_L) (1 - \cos^2 \theta_K) (2 \cos^2 \theta_\ell - 1) + \right. \\ \left. S_3 (1 - \cos^2 \theta_K) (1 - \cos^2 \theta_\ell) \cos 2\hat{\phi} + \right. \\ \left. \frac{4}{3} A_{FB} (1 - \cos^2 \theta_K) \cos \theta_\ell + \right. \\ \left. A_{Im} (1 - \cos^2 \theta_K) (1 - \cos^2 \theta_\ell) \sin 2\hat{\phi} \right],$$

where A_{FB} is forward backward asymmetry of the dimuon system, F_L is the fraction of longitudinal polarization of the K^{*0} , S_3 is proportional to the transverse asymmetry and A_{Im} is formed from the imaginary components of the transversity amplitudes of the K^{*0} .

For this analysis 1 fb^{-1} of data recorded by LHCb during the 2011 has been used. Events have been selected applying a soft selection exploiting the geometrical and kinematic properties of the events. A multivariate discriminant is also applied to improve the background rejection giving a S/B ratio of three in a $100 \text{ MeV}/c^2$ mass window around the B^0 mass. The selection criteria are designed to minimize the effects on the angular acceptance. After the application of the selection 900 ± 34 events have been observed, more than the sum of the events observed by BABAR[19], Belle [20] and CDF [21] collaborations. The effect of the acceptance to the angular distribution has been corrected using $B^0 \rightarrow K^{*0} J/\psi$ decays and comparing the data and MC samples. The data sample has been split in six q^2 bins. For the extraction of the four parameter A_{FB} , F_L , A_{Im} and S_3 , an unbinned maximum likelihood fit has been performed to the angular distribution and the invariant mass of $K^+ \pi^- \mu^+ \mu^-$. The background contribution is taken into account into the fit. Contribution from the $K^+ \pi^-$ S-wave is accounted for in the systematic error.

The results of the fit are reported in Fig.4, compared to theoretical predictions[23]. No SM prediction have been included for the region between the $c\bar{c}$ resonances where the prediction breaks down. The A_{FB} zero-crossing point in q^2 has been also measured. This values is well predicted in the SM, since it is largely free from form-factor uncertainties. This point has been extracted using an unbinned maximum likelihood fit to $K^+ \pi^- \mu^+ \mu^-$ and q^2 . The zero-crossing point is measured to be $q_0^2 = (4.9_{-1.3}^{+1.1}) \text{ GeV}^2/c^4$, to be compared with the SM predictions in the range $4.0 - 4.3 \text{ GeV}^2/c^4$.

¹ $\hat{\phi} = \phi + \pi$ if $\phi < 0$ and $\hat{\phi} = \phi$ if $\phi \geq 0$

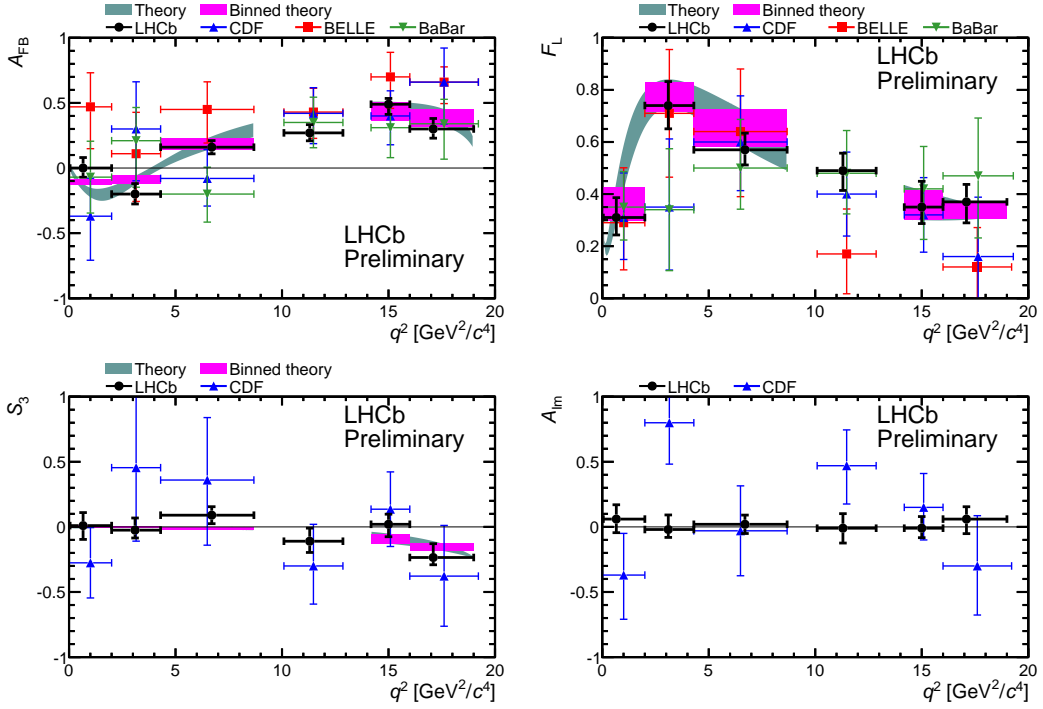


Figure 4: The forward backward asymmetry of the dimuon system A_{FB} (top-left), the fraction of longitudinal polarization of the K^{*0} F_L (top-right), the transverse asymmetry S_3 (bottom-left) and A_{Tm} (bottom-right) as a function of q^2 . Data points are reported in black for LHCb. *BaBar*, *Belle* and *CDF* data points are reported as comparison. Theoretical predictions are superimposed.

6. Isospin asymmetry in $B \rightarrow K^{(*)}\mu^+\mu^-$ decay

The isospin asymmetry is defined as follows:

$$A_I = \frac{\mathcal{B}(B^0 \rightarrow K^{(*)0}\mu^+\mu^-) - \frac{\tau_0}{\tau_+}\mathcal{B}(B^+ \rightarrow K^{(*)+}\mu^+\mu^-)}{\mathcal{B}(B^0 \rightarrow K^{(*)0}\mu^+\mu^-) + \frac{\tau_0}{\tau_+}\mathcal{B}(B^+ \rightarrow K^{(*)+}\mu^+\mu^-)}$$

where $\mathcal{B}(B \rightarrow f)$ is the branching fraction of the $B \rightarrow f$ decay and τ_0/τ_+ is the ratio of the lifetimes of the B^0 and B^+ . A_I is a theoretically clean observable because the leading form factor uncertainties cancel out. The SM expectation of this quantity for the $B \rightarrow K^*\mu^+\mu^-$ is -1% in the q^2 region below the J/ψ resonance, apart the very low region around $q^2 \sim 0$ where it rises to $\mathcal{O}(10\%)$ [24], while there is no precise prediction for the $B \rightarrow K\mu^+\mu^-$ decay. The measurement described in this section has been performed with 1fb^{-1} collected by LHCb during year 2011. The events are selected depending on the kaon decaying region with a cut-based or a multivariate discriminant selection. Both the selections use geometrical and kinematic information of the B candidate and of its daughters. The charged and the neutral channels have been selected using similar criteria in order to minimize systematic effects. An additional veto cut has been applied on the dimuon invariant mass in order to remove the J/ψ and $\psi(2S)$ resonances. The signal yields has been determined using an unbinned maximum likelihood fit to the $K^{(*)}\mu^+\mu^-$ invariant mass in the range $5170 - 5700\text{MeV}/c^2$. The fits are performed in six q^2 bins and over

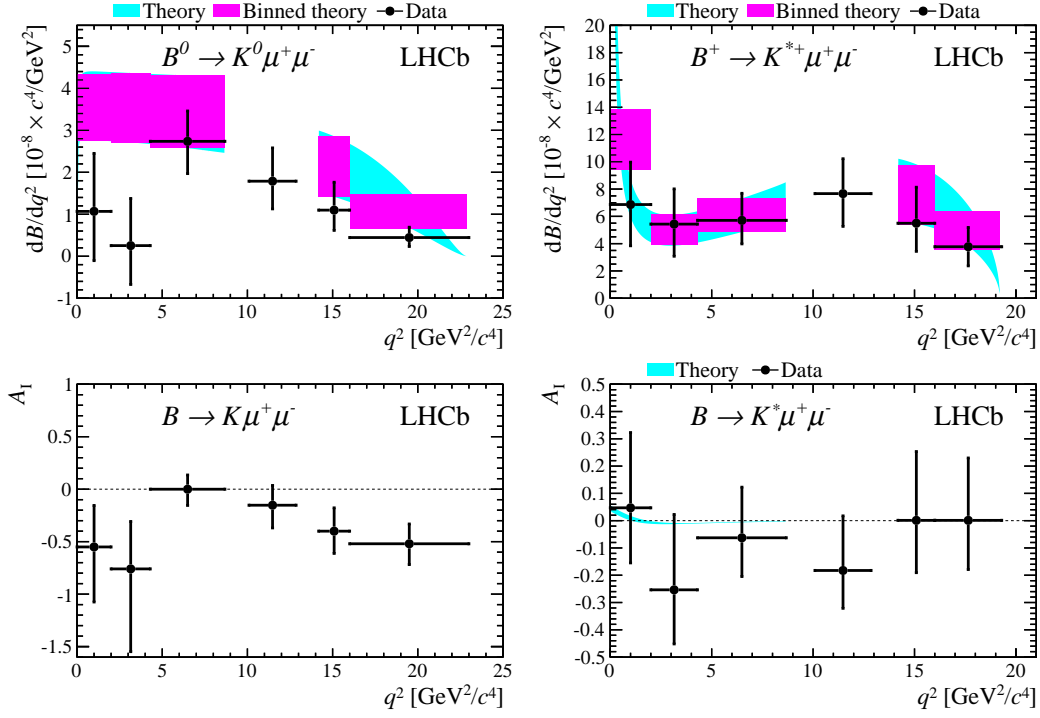


Figure 5: Differential branching fractions of $B^0 \rightarrow K^0 \mu^+ \mu^-$ (top-left) and $B^+ \rightarrow K^{*+} \mu^+ \mu^-$ with the theoretical SM predictions [25]. Isospin Asymmetry of $B \rightarrow K \mu^+ \mu^-$ (bottom-left) and $B \rightarrow K^* \mu^+ \mu^-$ bottom-right with its SM prediction

the full range. In order to reduce the systematic uncertainties, each signal mode is normalized to the $B \rightarrow J/\psi(\rightarrow \mu^+ \mu^-) K^{(*)}$ channel. The differential branching fractions are measured for $B^0 \rightarrow K^0 \mu^+ \mu^-$ and $B^+ \rightarrow K^{*+} \mu^+ \mu^-$ and are shown in Fig.5. Theoretical predictions are superimposed in high and low q^2 regions far from the $c\bar{c}$ resonances.

In Fig.5 the isospin asymmetry of $B \rightarrow K \mu^+ \mu^-$ and $B \rightarrow K^* \mu^+ \mu^-$ are shown. In the q^2 region below $4.3 \text{ GeV}^2/c^2$ and in the region above $16 \text{ GeV}^2/c^2$, A_I is negative in the $B \rightarrow K \mu^+ \mu^-$ channel. This asymmetry is dominated by a deficit in the observed $B^0 \rightarrow K^0 \mu^+ \mu^-$ signal. The total deviation from zero integrated over the whole q^2 range is equal to 4.4σ . The A_I in the $B \rightarrow K^* \mu^+ \mu^-$ case agrees with the SM prediction [25].

7. First observation of $B^+ \rightarrow \pi^+ \mu^+ \mu^-$

In the SM the $b \rightarrow d \ell^+ \ell^-$ transition is even more suppressed than $b \rightarrow s \ell^+ \ell^-$, by a factor $|V_{td}|/|V_{ts}|$. Furthermore, this process has never previously been observed. The predicted SM branching fraction for $B^+ \rightarrow \pi^+ \mu^+ \mu^-$ is $(1.96 \pm 0.21) \times 10^8$ [26]. However, many new physics models predict enhanced branching fractions for this decay [27]. The best limit has been published by Belle and it is $\mathcal{B}(B^+ \rightarrow \pi^+ \mu^+ \mu^-) < 6.9 \times 10^{-8}$ at 90% of C.L. [28]

The analysis performed by LHCb is based on a sample of 1.0 fb^{-1} of data collected in 2011.

The selection is based on a multivariate discriminant (BDT), trained using the kinematic properties of the daughters and the vertex quality of the B candidate. The J/ψ and $\psi(2S)$ resonances

are excluded using a veto on the dimuon mass.

The signal yields extracted from the fit is $25.3^{+6.7}_{-6.4}$. This result corresponds to an excess of 5.2σ with respect to the null hypothesis and consequently it represents the first observation of a $b \rightarrow d\ell^+\ell^-$ decay. Normalizing the observed signal to the $B^+ \rightarrow J/\psi K^+$ decay, LHCb obtained:

$$\mathcal{B}(B^+ \rightarrow \pi^+\mu^+\mu^-) = (2.4 \pm 0.6(\text{stat}) \pm 0.2(\text{syst})) \times 10^{-8}$$

which is in agreement with the SM expectation [29].

8. Conclusion

LHCb has demonstrated its power in many flavour physics topics, e.g. CPV studies with b and c hadrons, rare B and D decays and spectroscopy. We have presented some of the rare decays analyses based on 1 fb^{-1} collected by LHCb during year 2011.

The results on the upper limits on $\mathcal{B}(B^0 \rightarrow \mu^+\mu^-)$ and $\mathcal{B}(B_s^0 \rightarrow \mu^+\mu^-)$ put severe constraints on NP. Further improvements are foreseen with the analysis of the data sample that will be collected in year 2012. The combination of the upper limits obtained by ATLAS, CMS and LHCb has been also reported. This combination improves on the limits obtained by the individual experiments and represents the best existing limits on these decays. LHCb has also measured the upper limit on $\mathcal{B}(D^0 \rightarrow \mu^+\mu^-)$ which improves the current best published upper limit of about an order of magnitude. A search for the decays $B_s^0 \rightarrow \mu^+\mu^-\mu^+\mu^-$ and $B^0 \rightarrow \mu^+\mu^-\mu^+\mu^-$ is also discussed and the upper limits on their branching fractions are reported.

LHCb has also measured the differential branching fractions and the angular observables of the $B \rightarrow K^{*0}\mu^+\mu^-$ process. These are the most precise measurements of these quantities up to date and they are consistent with the SM predictions. The study of the isospin asymmetry A_I for the $B \rightarrow K^{(*)}\mu^+\mu^-$ process is reported. A 4σ deviation from the SM expectation has been observed for the $B \rightarrow K\mu^+\mu^-$ decays. This discrepancy is not observed in $B \rightarrow K^*\mu^+\mu^-$ case which agrees with the SM prediction. Moreover LHCb has clearly observed for the first time the $B^+ \rightarrow \pi^+\mu^+\mu^-$ decay. The evaluated branching fraction is in agreement with SM model expectation.

Many improvements are foreseen in the near future. With the 2012 run LHCb expects to double the data statistics and becomes even more competitive in constraining the phase spaces of NP models.

References

- [1] A. J. Buras, M. V. Carlucci, S. Gori, G. Isidori, *Higgs mediated FCNCs, Natural Flavour Conservation vs. Minimal Flavour Violation*, *JHEP* **1010** (2010) 009.
- [2] C. Hamzaoui, M. Pospelov and M. Toharia, *Higgs-mediated FCNC in supersymmetric models with large $\tan\beta$* , *Phys. Rev.* **D59** (1999) 095005;
- [3] R. Aaij et al. (LHCb Collaboration), *Strong Constraints on the Rare Decays $B_s^0 \rightarrow \mu^+\mu^-$ and $B^0 \rightarrow \mu^+\mu^-$* , *Phys. Rev. Lett.* **108** (2012) 231801 [[arXiv:1203.4493v2](#)].
- [4] A. Read, *Presentation of search results: the CL_s technique*, *J. Phys.* **G28** (2002) 2693.
- [5] K. de Bruyn et al., *On Branching Ratio Measurements of B_s Decays*, [[arXiv:1204.1735](#)].

- [6] T. Aaltonen et al. (CDF collaboration), *Search for $B_s^0 \rightarrow \mu^+ \mu^-$ and $B^0 \rightarrow \mu^+ \mu^-$ decays with CDF II*, Phys. Rev. Lett. **107** (2011) 191801, [arXiv:1107.2304].
- [7] S. Chatrchyan et al. (CMS Collaboration), *Search for $B_s^0 \rightarrow \mu^+ \mu^-$ and $B^0 \rightarrow \mu^+ \mu^-$ decays*, JHEP **1204** (2012) 033, [arXiv:1203.3976].
- [8] G. Aad et al. (ATLAS Collaboration), *Search for the decay $B_s^0 \rightarrow \mu^+ \mu^-$ with the ATLAS detector*, [arXiv:1204.0735].
- [9] R. Aaij et al. (LHCb Collaboration), *Search for the rare decays $B_s \rightarrow \mu^+ \mu^-$ and $B_d \rightarrow \mu^+ \mu^-$* , Phys. Lett. **B699** (2011) 330, [arXiv:1103.2465].
- [10] ATLAS Collaboration, CMS Collaboration and LHCb Collaboration, *Search for the rare decays $B_{(s)}^0 \rightarrow \mu^+ \mu^-$ at the LHC with the ATLAS, CMS and LHCb experiments*, CERN-LHCb-CONF-2012-017.
- [11] G. Burdman, E. Golowich, J. L. Hewett, and S. Pakvasa, *Rare charm decays in the Standard Model and beyond*, Phys. Rev. **D66** (2002) 014009, [arXiv:hep-ph/0112235].
- [12] E. Golowich, J. Hewett, S. Pakvasa, and A. A. Petrov, *Relating D^0 -anti- D^0 Mixing and $D^0 \rightarrow \ell^+ \ell^-$ with New Physics*, Phys. Rev. **D79** (2009) 114030, [arXiv:0903.2830].
- [13] Belle, M. Petric et al., *Search for leptonic decays of D^0 mesons*, Phys. Rev. **D81** (2010) 091102, [arXiv:1003.2345].
- [14] LHCb Collaboration, *Search for the $D^0 \rightarrow \mu^+ \mu^-$ decay with 0.9 fb^{-1} at LHCb*, LHCb-CONF-2012-005.
- [15] w D. Melikhov and N. Nikitin, *Rare radiative leptonic decays $B_{d,s} \rightarrow \mu^+ \mu^- \gamma$* , Phys. Rev. **D70**, (2004) 114028.
- [16] LHCb Collaboration, *Search for the rare decays $B_s^0 \rightarrow \mu^+ \mu^- \mu^+ \mu^-$ and $B^0 \rightarrow \mu^+ \mu^- \mu^+ \mu^-$* , LHCb-CONF-2012-010.
- [17] W. Altmannshofer et al., *Symmetries and Asymmetries of $B \rightarrow K^* \mu^+ \mu^-$ Decays in the Standard Model and Beyond*, JHEP **01** (2009) 019, [arXiv:0811.1214].
- [18] C. Bobeth, G. Hiller, and G. Piranishvili, *CP Asymmetries in $\bar{B} \rightarrow \bar{K}^* (\rightarrow \bar{K} \pi) \bar{\ell} \ell$ and Untagged $\bar{B}_s, B_s \rightarrow \phi (\rightarrow K^+ K^-) \bar{\ell} \ell$ Decays at NLO*, JHEP **0807** (2008) 106, [arXiv:0805.2525].
- [19] S. Akar, *Radiative penguin results from BABAR*, talk at Lake Louise Winter institute 2012.
- [20] Belle collaboration, J.-T. Wei et al., *Measurement of the Differential Branching Fraction and Forward-Backward Asymmetry for $B^0 \rightarrow K^{*0} \ell^+ \ell^-$* , Phys. Rev. Lett. **103** (2009) 171801.
- [21] CDF collaboration, T. Aaltonen et al., *Measurements of the Angular Distributions in the Decays $B \rightarrow K^{(*)} \mu^+ \mu^-$ at CDF*, Phys. Rev. Lett. **108** (2012) 081807, [arXiv:1108.0695].
- [22] LHCb Collaboration, *Differential branching fraction and angular analysis of the $B^0 \rightarrow K^{*0} \mu^+ \mu^-$ decay*, LHCb-CONF-2012-008.
- [23] C. Bobeth, G. Hiller, and D. van Dyk, *More Benefits of Semileptonic Rare B Decays at Low Recoil: CP Violation*, [arXiv:1105.0376].
- [24] T. Feldmann and J. Matias, *Forward-backward and isospin asymmetry for $B \rightarrow K^{(*)} \ell^+ \ell^-$ decay in the Standard Model and in supersymmetry*, JHEP **01** (2003) 074, [arXiv:hep-ph/0212158].
- [25] LHCb Collaboration, *Measurement of the isospin asymmetry in $B \rightarrow K^{(*)} \mu^+ \mu^-$ decays*, CERN-PH-EP-2012-129.
- [26] H.-Z. Song, L.-X. Lü, and G.-R. Lu, *New physics effects on rare decays $B^+ \rightarrow \pi^+ \ell^+ \ell^-$, $\rho^+ \ell^+ \ell^-$ in a top quark two-higgs-doublet model*, Communications in Theoretical Physics **50** (2008) 696.
- [27] J.-J. Wang, R.-M. Wang, Y.-G. Xu, and Y.-D. Yang, *The Rare decays $B^+ \rightarrow \pi^+ \ell^+ \ell^-$, $\rho^+ \ell^+ \ell^-$, $B^0 \rightarrow \mu^+ \mu^-$ in the R-parity violating supersymmetry*, Phys. Rev. **D77** (2008) 014017, [arXiv:0711.0321].
- [28] Belle collaboration, J.-T. Wei et al., *Search for $B^+ \rightarrow \pi^+ \ell^+ \ell^-$ Decays at Belle*, Phys. Rev. **D78** (2008) 011101, [arXiv:0804.3656].
- [29] LHCb Collaboration, *First observation of $B^+ \rightarrow \pi^+ \mu^+ \mu^-$* , LHCb-CONF-2012-006.